

# NEW GREEN POLYMER COMPOSITES PROCESSED BY ADDITIVE MANUFACTURING FOR "CLEAN SPACE" APPLICATION

M. Rinaldi<sup>1,3</sup>, I. Cacciotti<sup>2,3</sup>, T. Ghidini<sup>4</sup>, L. Pambaguian<sup>4</sup>, U. Lafont<sup>4</sup>, V. Canala<sup>5</sup>, V. Massarelli<sup>5</sup>, F. Nanni<sup>1,3</sup>

<sup>1</sup>University of Rome "Tor Vergata", Via del Politecnico1, 00133 Rome, Italy

<sup>2</sup>University of Rome "Niccolò Cusano", Via Don Carlo Gnocchi 3, 00166 Rome, Italy

<sup>3</sup>Italian Interuniversity Consortium on Materials Science and Technology (INSTM), Italy

<sup>4</sup>European Space Agency - ESA/ESTEC, Materials Technology Section, Noordwijk, The Netherlands/Pays Bas

<sup>5</sup>Mecaer Aviation Group, Via dell'artigianato 1, 63076 Monteprandone (AP), Italy

## ABSTRACT

*Additive Layer Manufacturing (ALM) technology is an intrinsically green technology as it often allows using less material than when using conventional manufacturing techniques. A major contribution to satellite demissability could be achieved by using ALM and substituting metals with polymers. Indeed, these materials have low melting temperature and would likely burn during atmospheric re-entry. Therefore together with the development of ALM technologies, the range of polymeric materials available for such process needs to be increased. In this work new polymer bio-composites were developed, using as polymeric matrix polyetherimide (PEI), a high performance thermoplastic, and as natural filler diatomaceous earth, both uncalcined and calcined. Moreover uncalcined diatomite was also amino-functionalized, in order to increase its chemical compatibility with the matrix.*

*Mechanical test and microstructural characterization were performed to evaluate the influence of the filler content (i.e. 1-10 % wt) and of different diatomite varieties on the composites performance. The collected results show an increase of Young Modulus with the filler content, particularly in the case of untreated diatomite, both pristine and amino-functionalised, suggesting a good chemical compatibility between filler and matrix. This is substantiated by the scanning electron microscopy (SEM) observation of the fracture surface of samples after tensile test.*

## INTRODUCTION

Additive Layer Manufacturing (ALM) technology has been successfully applied during the last years in numerous applications, not only for rapid prototyping purpose, but also to realize functional components in different industrial sectors including aerospace, automotive and medical ones.

Scientific and industrial interest for ALM technology is constantly increasing, although at present, the choice of ALM processable polymers is relatively limited, particularly in the case of fused deposition modelling (FDM) technology. FDM is one of the most widely used methods for fabricating thermoplastic parts with low cost and minimal wastage [1,2].

Currently, only thermoplastic filaments are used as feedstock in FDM including acrylonitrile butadiene styrene (ABS), polycarbonate (PC), polylactide (PLA), polyamide (PA). Recently Stratasys has begun to produce wires made of polyetherimide (PEI) [3], with incremented mechanical properties, opening new fields of applications for FDM.

Therefore together with the development of ALM technologies [4], the range of materials suitable for such process needs to be increased [5].

Furthermore, there is a growing attention towards the development of innovative composites and nano-composites [6], based on biodegradable materials. Among them, polymeric matrix bio-based composites reinforced by natural fillers and characterised by an optimal filler/matrix interaction could be designed for prospective applications in automotive, aerospace and packaging industries [7,8]. In this manner, they would present an improvement in terms of both performance and environmental aspects [9]. The basic idea is to develop new green composite materials based on polymers with a good Life Cycle Assessment (LCA) and appropriate fillers, looking for raw materials of natural origin and then easily disposable to limit and confine pollution [10]. In particular, there is a great attention on the availability of bio-based fillers, such as banana, hemp, cellulose [11], coconut fibers [12], nanoclays, diatomite, to insure some degree of recycle.

Bioderived fibers offer limited mechanical properties and thermal stability, whereas inorganic ceramic natural particles present good thermal and mechanical properties [11,13].

In this framework, the purpose of the present work was to develop an innovative polymeric matrix composite, composed of a conventional thermoplastic polymer commonly used in aerospace application, i.e. polyetherimide (PEI), and a natural inorganic filler, i.e. the diatomaceous earth.

It is important to underline that, to the best of our knowledge, this polymer has not been reinforced with natural fillers yet, but only with glass and carbon microfibers and with nanosilica [14].

As polymeric matrix, PEI was selected, being a high-performance thermoplastic polymer with good heat resistance, excellent mechanical properties, inherent flame resistance and solvent resistance [15]. Recent NASA studies have demonstrated that it is possible to obtain PEI without the use of any hazardous solvent, enabling to employ this polymer as a greener choice [16]. Furthermore, up to now, the biobased polymers (e.g. polylactic acid, polyhydroxyalkanoates...) have rather low mechanical properties [17], some of them are difficult to be machined with the usual production techniques, and in any case they can not to be used for space application due to outgassing and ageing problems, according to ECSS standards [18].

As inorganic filler, the diatomaceous earth, a fossil flour of sedimentary origin, composed of fragments of diatom siliceous skeletons ("frustules") with different sizes (ranging from 2  $\mu\text{m}$  to 2 mm) and shapes (e.g. rounded, elongated,...), was chosen, due to its large availability in many areas of the world, chemical resistance, non-toxicity, high porosity and bulk volume, large specific surface area (up to 200  $\text{m}^2/\text{g}$ ) [19]. The main constituent of diatomite is amorphous silica, although it can contain impurities such as organic components and metallic oxides ( $\text{MgO}$ ,  $\text{Al}_2\text{O}_3$ ,  $\text{Fe}_2\text{O}_3$ ) coming from environment [20]. For all these properties, these fossil structures have been widely used in a lot of industrial applications, such as food production, water extracting agent, production of cosmetics and pharmaceuticals [21].

Thus the present research is aimed to set up the optimal composition of this innovative composite material, based on PEI and diatomite, to be potentially used for FDM ALM manufacturing process. In order to achieve this objective, PEI films loaded with different diatomite contents, ranging between 1 % wt/wt and 10 % wt/wt with respect to the polymer, were prepared by solvent casting technique. Both uncalcined and calcined diatomites were used and compared, to evaluate the influence of different morphologies and crystalline phases of the employed fillers on the microstructural and on the mechanical properties of the composites. To improve the compatibility between the polymeric matrix and the filler, the uncalcined diatomite was also organosilane-modified.

## EXPERIMENTAL

### Amino-functionalization of the calcined diatomite

1g of calcined diatomaceous earth powder (Celite® S, untreated, composition:  $\text{Al}_2\text{O}_3$  4.1%,  $\text{CaO}$ , 0.4%,  $\text{Fe}_2\text{O}_3$ , 1.6%,  $\text{MgO}$ , 0.2%,  $\text{Na}_2\text{O} + \text{K}_2\text{O}$ , 1.4%,  $\text{P}_2\text{O}_5$ , 0.3%,  $\text{SiO}_2$ , 90.2%,  $\text{TiO}_2$ , 0.2% *Sigma Aldrich*) was added to a mixture composed by 8 ml of Aminopropyldiethoxymethylsilane (APDEMS, *Sigma Aldrich*), used as silane coupling agent, and 200 ml of toluene, and magnetically stirred for 24 h at room temperature [22] (**Figure 1**).

Then the suspension was vacuum filtered and the obtained powder was washed several times with toluene to remove the unreacted silane.

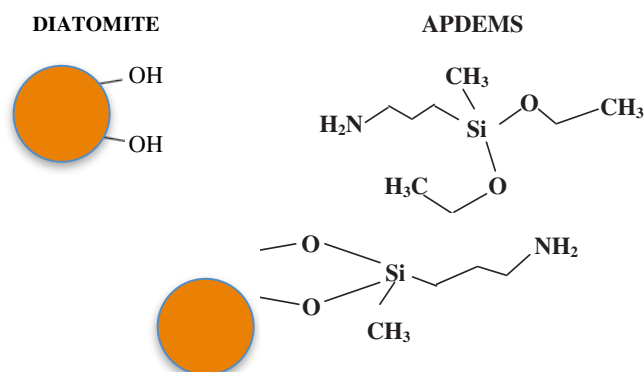


**Figure 1** Schematic of amino-functionalization of uncalcined diatomite using a silane coupling agent

### Preparation of PEI/diatomite films by solvent casting

Firstly, dispersions of the used fillers (i.e. uncalcined (DE), amino-functionalised (FDE) and calcined diatomite (CDE, *Supercell Fine*, average size 14  $\mu\text{m}$ , composition:  $\text{Al}_2\text{O}_3$  4.0%,  $\text{CaO}$  0.5%,  $\text{Fe}_2\text{O}_3$  1.3%,  $\text{Na}_2+\text{K}_2\text{O}$  1.1%,  $\text{SiO}_2$  91.1%, *Sigma Aldrich*)) were prepared by suspending the particles in chloroform ( $\text{CHCl}_3$ ) and sonicating them for 1 hour in an ultrasound bath.

Different weight percentages of fillers (i.e. 1, 3, 5, 10 wt.% with respect to the polymer) were investigated. Pellets of polyetherimide (PEI, melt index: 9 g/10 min (337  $^\circ\text{C}$ /6.6kg), density: 1.27 g/mL at 25  $^\circ\text{C}$ ) were added to the prepared suspensions to obtain the targeted composition (i.e. PEI concentration of 5 % wt/wt with respect to the solvent, Table 1).

**Table 1** Nomenclature and composition of the prepared composite films

SAMPLE	Filler	%weight of filler
PEI NEAT		
PEI/1CDE	Diatomite	1%
PEI/3CDE	Diatomite	3%
PEI/5CDE	Diatomite	5%
PEI/10CDE	Diatomite	10%
PEI/1DE	Celite S	1%
PEI/3DE	Celite S	3%
PEI/5DE	Celite S	5%
PEI/10DIE	Celite S	10%
PEI/1FDE	Amino-functionalised Celite S	1%
PEI/3FDE	Amino-functionalised Celite S	3%
PEI/5FDE	Amino-functionalised Celite S	5%
PEI/10FDE	Amino-functionalised Celite S	10%

As a reference, neat PEI film was also prepared following the same procedure. Figure 2 shows the mechanism behind the chemical bond formation between functionalized diatomite and PEI. Finally the obtained suspensions were cast on a teflon Petri and maintained under fumehood for around 2-3 days in order to completely evaporate the solvent.

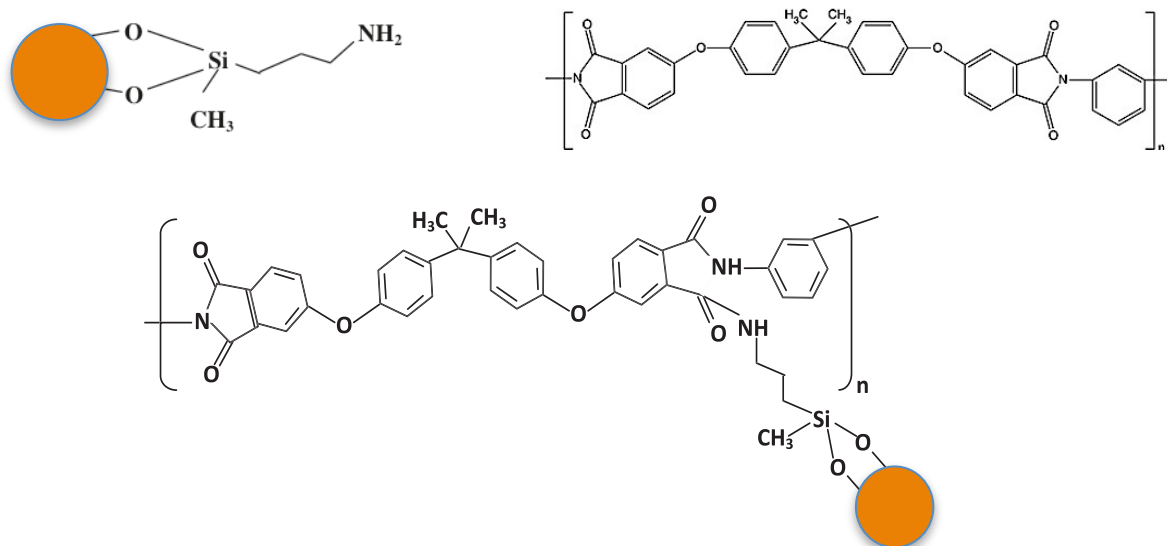


**Figure 2 Schematic of chemical bond formation between functionalized diatomite and PEI**

### Characterization techniques

The morphology of both the used fillers and the produced films was analysed by means of scanning electron microscopy (FE-SEM, *Cambridge Leo Supra 35*).

The characteristic chemical groups of the uncalcined diatomite powder, before and after the amino-functionalisation, were investigated by Fourier Transform Infrared Spectroscopy (FTIR, *Spectrum 100 Optica, Perkin Elmer*) in the following conditions: wavenumber range  $400\text{--}4000\text{ cm}^{-1}$ , spectral resolution  $4\text{ cm}^{-1}$ . The mechanical properties of the prepared films were investigated by means of uniaxial tensile tests on dog-bone specimens (width 4.8 mm, length 22.25 mm), at 1.2 mm/min up to rupture. These test were carried out through an electromechanical machine equipped with a 500 N load cell (Lloyd LRX), following the ASTM D1708 and D638 standards. Finally, the fracture surface of the samples after the tensile test was investigated by means of scanning electron microscopy (FE-SEM, *Cambridge Leo Supra 35*), to investigate the distribution of the fillers within the polymeric matrix and the compatibility between the inorganic and the organic components.

## RESULTS AND DISCUSSION

In **Figure 3** the SEM micrographs of the uncalcined and calcined diatomites are reported.

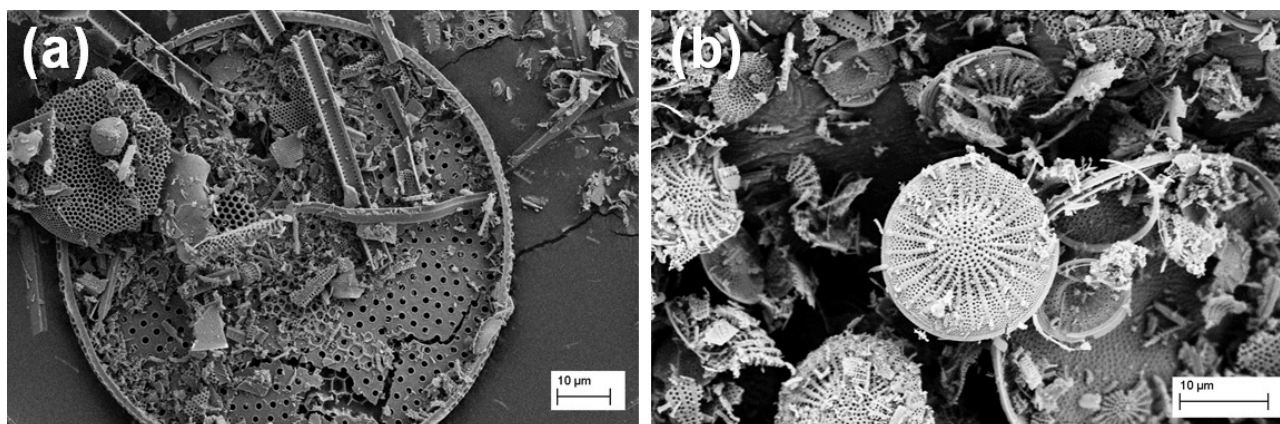


**Figure 3** SEM micrographs of calcined (a) and uncalcined (b) diatomite

The calcined diatomite is composed of particles of different shapes (i.e. rounded, elongated,...) and dimensions (between 2 and 70-80  $\mu\text{m}$ ). It is interesting to note that all particles present a hierarchical porosity, with pore dimension ranging from few micrometres down to few tens nanometres.

The uncalcined diatomite shows a more uniform and homogeneous distribution in size and shape, with similar hierarchical porosity characteristics.

The amino-functionalisation was demonstrated by FT-IR investigation. In Figure 4 the FT-IR spectra of the uncalcined diatomite before and after the amino-functionalisation are displayed.

In both spectra the typical vibrational modes of silica were detected (Figure 4a), such as the peaks at 470, 800 and 1100  $\text{cm}^{-1}$  that correspond to the Si-O-Si bending mode, Si-O stretching mode of [Si-O-Si], and asymmetric stretching mode of Si-O-Si bonds, respectively [23].

The broad band around 3400  $\text{cm}^{-1}$  and the peak at 1636  $\text{cm}^{-1}$  are associated to OH vibration mode of the physically adsorbed  $\text{H}_2\text{O}$  and bending vibration of water molecules retained in the diatomite silica matrix [24].

In the case of the pristine uncalcined powder, the peak at 917  $\text{cm}^{-1}$  corresponds to (Si-O) stretching of silanol group (Si-OH). This peak is not detectable in the case of organosilane-modified powder, showing that functionalisation occurred. This observation is further supported by the presence of additional peaks at 1470, 1542 and 1575, 2917 and 2850  $\text{cm}^{-1}$ .

In details, the peaks at 2917 and 2850  $\text{cm}^{-1}$  (Figure 4b) are ascribed to the asymmetric and symmetric stretching modes of the  $-\text{CH}_2-$  moiety, respectively, which is directly related to the carbon chain of organosilane molecules [25].

The peaks at 1575  $\text{cm}^{-1}$  and 1470  $\text{cm}^{-1}$  are due to the  $-\text{NH}_2$  terminal group and the  $-\text{NH}_3^+$  group, respectively (Figure 4a). Both these modes are associated with the  $-\text{NH}_2$  groups from APDMES [26]. In conclusion, these FTIR results clearly demonstrate the presence of  $-\text{NH}_2$  and  $-\text{CH}_3$  functional groups on the diatom surface originating from the used silane and the effectiveness of the silanization procedure.

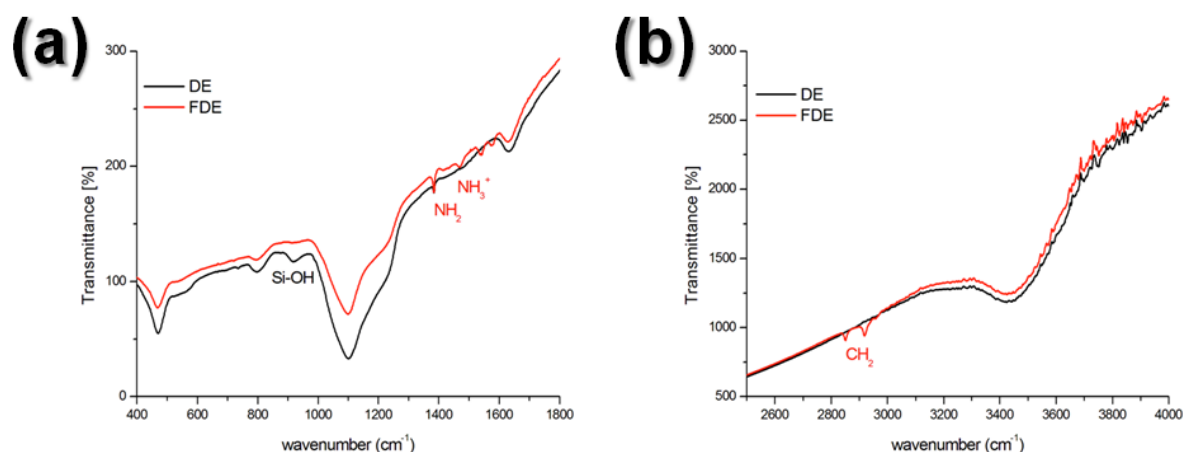


**Figure 4** FT-IR spectra of the uncalcined diatomite before and after the amino-functionalisation: (a) between 400 and 1800  $\text{cm}^{-1}$ ; (b) between 2500 and 4000  $\text{cm}^{-1}$ .

Regarding the mechanical characterisation, the  $\sigma$ - $\epsilon$  curves of films loaded with different amount of filler are reported in Figure 5. The mechanical properties are summarized in terms of ultimate tensile strength ( $\sigma_{\max}$ ), Young's modulus (E), Young's modulus variation with respect to neat sample ( $\Delta E$  [%]), and elongation at break ( $\epsilon_{\max}$ ) in Table 2.

**Table 2** Tensile modulus (E), ultimate tensile stress ( $\sigma_{\max}$ ), elongation at break ( $\epsilon_{\max}$ ) and Young modulus variation with respect to neat sample of all tested films (all values are expressed as mean values $\pm$ standard deviation (SD)).

	$\sigma$ [MPa]	E [GPa]	$\Delta E$ [%]	$\epsilon_{\max}$ [%]
PEI NEAT	45 $\pm$ 3	1.272 $\pm$ 0.01	-	9
PEI/1CDE	40 $\pm$ 7	1.488 $\pm$ 0.01	17	14
PEI/3CDE	44 $\pm$ 3	1.324 $\pm$ 0.28	4	17
PEI/5CDE	45 $\pm$ 3	1.312 $\pm$ 0.07	3	9
PEI/10CDE	46 $\pm$ 3	1.483 $\pm$ 0.14	17	6
PEI/1DE	44 $\pm$ 1	1.531 $\pm$ 0.11	20	15
PEI/3DE	46 $\pm$ 3	1.400 $\pm$ 0.01	10	18
PEI/5DE	48 $\pm$ 3	1.469 $\pm$ 0.03	15	6
PEI/10DE	43 $\pm$ 2	2.039 $\pm$ 0.01	60	4
PEI/1FDE	46 $\pm$ 1	1.551 $\pm$ 0.12	22	11
PEI/3FDE	47 $\pm$ 3	1.672 $\pm$ 0.07	28	4
PEI/5FDE	51 $\pm$ 1	1.740 $\pm$ 0.06	37	5
PEI/10FDE	44 $\pm$ 3	2.048 $\pm$ 0.02	61	3

An increase of the Young's modulus with the filler content was detected, especially for functionalised samples. The ultimate tensile strength seemed to be less significantly impacted by the filler type and content.

In Figure 5a the tensile curves of the films loaded with amino-functionalised diatomite at different contents are shown. It evidences a progressive increment of the stiffness value with the filler content, associated to a decreased elongation at break, as expected. It is interesting to note that in the case of high filler content and strong interfacial bond (PEI/10FDE) the mechanical response becomes brittle.

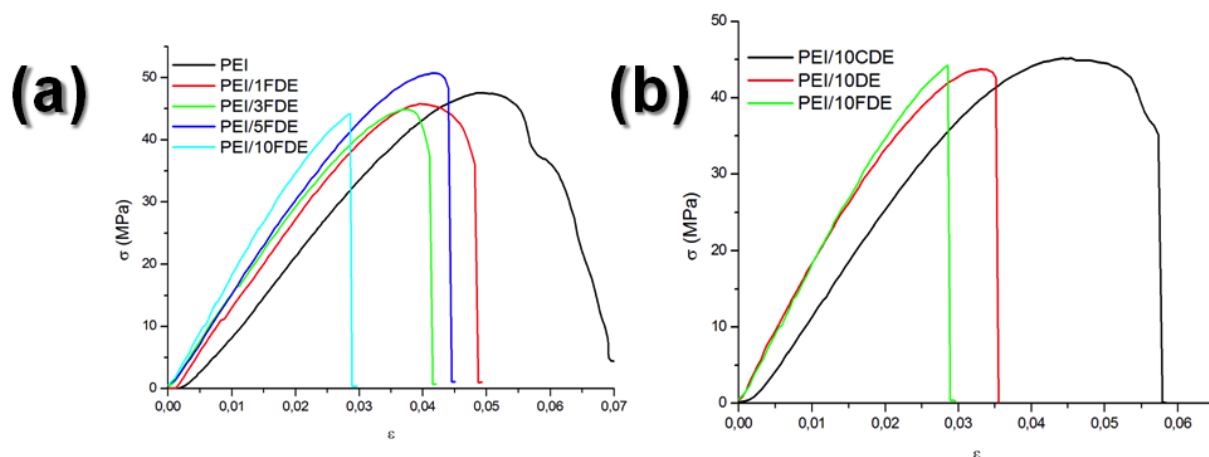


**Figure 5 Stress-Strain curves of PEI films loaded with: (a) amino-functionalised diatomite in different amounts (1-10 %wt); (b) 10 %wt of uncalcined, calcined and amino-functionalised diatomites.**

Comparing the data related to the uncalcined and calcined diatomites (Table 2, Figure 5b), it is possible to conclude that higher mechanical properties can be obtained in the first case, probably due to both the different and more homogeneous morphology and to the different crystalline phases of uncalcined powder. Moreover, as already underlined, the improved mechanical properties for the films loaded with amino-functionalised diatomite suggest a better bonding between filler and matrix with respect to unfunctionalised and calcined ones, even if a good filler wettability was obtained in all cases, as shown by the SEM observation of the fracture surface of stress strained films (Figure 5)

In fact, from the observation of the fracture surface of the stress-strained films after the tensile test, it is interesting to evidence that the micro-nano holes of diatomite structure were completely filled by the polymer confirming the good chemical compatibility (see Figure 5), independently from the kind of diatomite.

The not significantly altered ultimate tensile stress in the case of composite films with respect to the neat polymer is imputable to the employed process technology (i.e. solvent casting).

From the reported SEM micrographs, it is evident that the diatomite tended to sediment on the bottom of the Petri dish, generating a biphasic material, composed of a thicker polymeric layer and a thinner silica based layer with a low content of polymer that acts as a binder.

Obviously the thickness of the inorganic layer increases with the filler content, determining an increment of the Young modulus value, whereas the ultimate tensile strength seems to be mainly influenced by the polymeric layer.

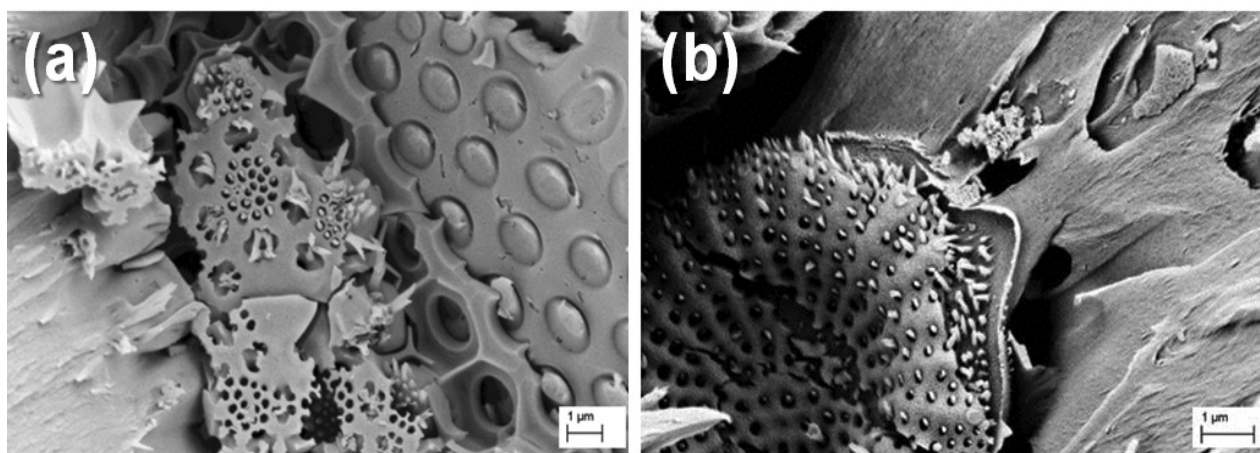


**Figure 5 SEM micrographs of the surface fracture of PEI films loaded with 5%wt of calcined (a) and uncalcined (b) diatomite.**

On the basis of the recorded mechanical properties, it is possible to conclude that the PEI/5FDE can be considered the optimal composition for the production of components by AL-FDM, since leads to a remarkable increment of the Young modulus value, maintaining a good ultimate tensile strength, with a inorganic filler content. In fact, in order to identify the composite composition for the production by ALM-FDM, it has to be taken into account many concomitant factors: not only the mechanical performances, but also the intrinsic chemical characteristic of the material to be processed, such as its viscosity in melted state that could be excessively incremented with too high contents of the inorganic filler.

## CONCLUSIONS

An innovative composite material based on polyetherimide as matrix and diatomaceous earth as filler was prepared investigating the effect of different filler concentration (i.e. 1-10 %wt) and of the surface functionalization of the diatomite (using APDEMS in order to obtain an amino-functionalisation to improve the chemical compatibility with PEI). Surface functionalization of filler was obtained and confirmed by FT-IR analysis, whereas the enhanced chemical compatibility between the polymeric matrix and the organosilane-modified filler was confirmed by the mechanical test results. However a good interfacial adhesion between diatomite and the matrix was achieved in all cases, independently from the diatomite kind, as evidenced by SEM observations of the fracture surface of stress strained films. Indeed, mechanical testing shows a progressive increment of the Young's modulus with the filler content, particularly evident for the films loaded with amino-functionalised powder, while the tensile strength is comparable to neat PEI matrix and does not seem significantly modified by the filler addition, due to the formation of a bilayer structure. Considering the final application (i.e. production of composites to be potentially used for FDM ALM manufacturing process), the compositions based on 5 %wt of diatomite was selected as the optimal one. Further studies should target an improved filler dispersion within the polymeric matrix, avoiding the deposition of the used fillers on the bottom of the petri dish, and investigate the lack of ultimate strength rising.

## REFERENCES

- [1] Stratasys Inc. Technical application guide: FDM for Jigs and Fixtures 2013  
[http://www.stratasys.com/media/main/secure/technical/ApplicationGuides-TAG/SSYS-TAG\\_JigsFixtures-](http://www.stratasys.com/media/main/secure/technical/ApplicationGuides-TAG/SSYS-TAG_JigsFixtures-)
- [2] Kai C, Fai LK, Chu-Sing L. Rapid prototyping: principles and applications in manufacturing. 2nd ed. Singapore: Word Scientific Publishing; 2003
- [3] <http://www.stratasys.com/materials/fdm/ultem-9085>
- [4] Christiane Beyer, Strategic Implications of Current Trends in Additive Manufacturing J. Manuf. Sci. Eng 136(6), 064701 (Oct 24, 2014)
- [5] Belvin W.K., Zander, M.E, Sleight D. W., Connell J., Holloway N., Palmieri F; Materials, Structures and Manufacturing: An Integrated Approach to Develop Expandable Structures, American Institute of Aeronautics and Astronautics Inc., AIAA Paper 2012-1951, NF1676L-13247.
- [6] Satish Joshi, Can Nanotechnology Improve the Sustainability of Biobased Products: The Case of Layered Silicate Biopolymer Nanocomposites, Journal of Industrial Ecology 2008, Volume 12, Issue 3, pp. 474–489
- [7] A. K. Mohanty, M. Misra, L. T. Drzal, Sustainable Bio-Composites from Renewable Resources: Opportunities and Challenges in the Green Materials World, Journal of Polymers and the Environment; April 2002, Volume 10, Issue 1-2, pp 19-26;
- [8] Avella, M.; Buzarovska, A.; Errico, M.E.; Gentile, G.; Grozdanov, A. Eco-Challenges of Bio-Based Polymer Composites. Materials 2009, 2, 911-925
- [9] F.P. La Mantia, M. Morrealeb; Review Green composites: A brief review; Composites Part A: Applied Science and Manufacturing, Volume 42, Issue 6, June 2011, Pages 579–588,
- [10] Michaelangelo D. Tabone et al. Sustainability Metrics: Life Cycle Assessment and Green Design in Polymers; Environ. Sci. Technol., 2010, 44 (21), pp. 8264–8269
- [11] Cacciotti, I.; Fortunati, E.; Puglia, D., Kenny, J. M.; Nanni, F., Effect of silver nanoparticles and cellulose nanocrystals on electrospun poly(lactic) acid mats: morphology, thermal properties and mechanical behaviour, Carbohydrate Polymers 2014, 103, pp. 22– 31.
- [12] V. Paula, K. Kannyb, G.G. Redhia Mechanical, thermal and morphological properties of a bio-based composite derived from banana plant source, Composites Part A: Applied Science and Manufacturing, Volume 68, January 2015, Pages 90–100
- [13] Al-Oqla et al. Selecting Natural Fibers for Bio-Based Materials with Conflicting Criteria American Journal of Applied Sciences 12.1 (2015): 64-71.



- [14] Bor-Kuan Chen et al. ; Preparation of Polyetherimide Nanocomposites with Improved Thermal, Mechanical and Dielectric Properties Polymer Bulletin 57, 671–681 (2006)
- [15] Johnson RO, Burlhis HS (1983) Polyetherimide: a new high-performance thermoplastic resin. J Polym Sci Polym Symp 70:129–143
- [16] NASA Patent US7015304 B1 SOLVENT FREE LOW-MELT VISCOSITY IMIDE OLIGOMERS AND THERMOSETTING POLYIMIDE COMPOSITES
- [17] Rolf Mülhaupt\*, Green Polymer Chemistry and Bio-based Plastics: Dreams and Reality, Macromolecular Chemistry and Physics, Volume 214, Issue 2, pages 159–174, January 25, 2013
- [18] ECSS-Q-ST-70-71C Materials, processes and their data selection [18] O. Şan, R. Gören, C. Özgür, Purification of diatomite powder by acid leaching for use in fabrication of porous ceramics, Int. J. Miner. Process. 93 (2009) 6–10.
- [19] Y. Wang, J. Cai, Y. Jiang, X. Jiang, D. Zhang, Preparation of biosilica structures from frustules of diatoms and their applications: current state and perspectives, Appl. Microbiol. Biotechnol. 97 (2013) 453–462.
- [20] Ilaria Rea et al. , Diatomite biosilica nanocarriers for siRNA transport inside cancer cells; Biochimica et biophysica acta 2014
- [21] High modulus high strength high flow osu compliant polyetherimide-carbon fiber composites for metal replacement US Patent 20130331505 A1
- [22] S. Takahashi D.R. Paul , Gas permeation in poly(ether imide) nanocomposite membranes based on surface-treated silica. Part 2: With chemical coupling to matrix Polymer 47 (2006) 7535e7547
- [23] Sheng G et al 2009 Colloids Surf. A 339 159; Huang J, Liu Y, Jin Q, Wang X and Yang J 2007 J. Hazard. Mater. 143 541.
- [24] L. Chen, J. Xu, J. Hu, J. Radioanal. Nucl. Chem. 297 (2012) 97–105.
- [25] Liang X, Xu Y, Sun G, Wang L, Sun Y and Qin X 2009 Colloid Surf. Physicochem. Eng. Aspect 349 61; Finocchio E, Macis E, Raiteri R and Busca G 2007 Langmuir 23 2505.
- [26] Maria Chong A S and Zhao X S 2003 J. Phys. Chem. B 107 12650.